Environmental Research Letters

ACCEPTED MANUSCRIPT • OPEN ACCESS

Multi-decadal shoreline change in coastal Natural World Heritage Sites – a global assessment

To cite this article before publication: Salma Sabour *et al* 2020 *Environ. Res. Lett.* in press https://doi.org/10.1088/1748-9326/ab968f

Multi-decadal shoreline change in coastal Natural World Heritage Sites – a global assessment

Salma Sabour[1], Sally Brown[2], Robert J. Nicholls[1, 3], Ivan D. Haigh[4], Arjen P. Luijendijk[5, 6]

[1]Faculty of Engineering and Physical Sciences, University of Southampton, Highfield, Southampton, SO17 1BJ, United Kingdom.
[2]Department of Life and Environmental Sciences, Bournemouth University, Fern Barrow, Bournemouth BH12 5BB, United Kingdom.
[3]Tyndall Centre for Climate Change Research, University of East Anglia, Norwich Research Park, Norwich NR4 7TJ, United Kingdom.
[4]School of Ocean and Earth Science, National Oceanography Centre Southampton, University of Southampton, Waterfront Campus, European Way, Southampton, SO14 3ZH, United Kingdom.
[5]Faculty of Civil Engineering and Geosciences, Delft University of Technology, Delft, The Netherlands
[6]Deltares, Delft, The Netherlands

May 2020

Abstract

Natural World Heritage Sites (NWHS), which are of Outstanding Universal Value, are increasingly threatened by natural and anthropogenic pressures. This is especially true for coastal NWHS, which are additionally subject to erosion and flooding. This paper assesses shoreline change from 1984 to 2016 within the boundaries of 67 designated sites, providing a first global consistent assessment of its drivers. It develops a transferable methodology utilising new satellite-derived global shoreline datasets, which are classified based on linearity of change against time and compared with global datasets of geomorphology (topography, land cover, coastal type, and lithology), climate variability and sea-level change. Significant shoreline change is observed on 14% of 52 coastal NWHS shorelines that show the largest recessional and accretive trends (means of -3.4 m yr^{-1} and 3.5 m yr^{-1}, respectively). These rapid shoreline changes are found in low-lying shorelines (< 1 m elevation) composed of unconsolidated sediments in vegetated tidal coastal systems (means of -7.7 m yr^{-1} and 12.5 m yr^{-1}), and vegetated tidal deltas at the mouth of large river systems (means of -6.9 and 11 m yr^{-1}). Extreme shoreline changes occur as a result of redistribution of sediment driven by a combination of geomorphological conditions with (1) specific natural coastal morphodynamics such as opening of inlets (e.g. Río Plátano Biosphere Reserve) or gradients of alongshore sediment transport (e.g. *Namib Sea*) and (2) direct or indirect human interferences with natural coastal processes such as sand nourishment (e.g. *Wadden Sea*) and damming of river sediments upstream of a delta (e.g. *Danube Delta).* The most stable soft coasts are associated with the protection of coral reef ecosystems (e.g. *Great Barrier Reef*) which may be degraded/destroyed by climate change or human stress in the future. A positive correlation between shoreline retreat and local relative sea-level change was apparent in the *Wadden Sea*. However, globally, the effects of contemporary sea-level rise are not apparent for coastal NWHS, but it is a major concern for the future reinforcing the shoreline dynamics already being observed due to other drivers. Hence, future assessments of shoreline change need to account of other drivers of coastal change in addition to sea-level rise projections. In conclusion, extreme multi-decadal linear shoreline trends occur in coastal NWHS and are driven primarily by sediment redistribution. Future exacerbation of these trends may affect heritage values and coastal communities. Thus shoreline change should be considered in future management plans where necessary. This approach provides a consistent method to assess NWHS which can be repeated and help steer future management of these important sites.

Keywords: shoreline change, multi-decadal, local and global scales, UNESCO, conservation, World Natural Heritage Sites, sea-level rise, coastal heritage, erosion, recession, accretion

1 Introduction

World Heritage Sites are locations of Outstanding Universal Values (OUV) selected by the United Nations Educational, Scientific and Cultural Organization (UNESCO) as having cultural, historical, scientific, or other forms of significance[1]. Of the 1 092 World Heritage Sites, 209 are classified as Natural World Heritage Sites (NWHS)[1]. NWHS have a high irreplaceability (uniqueness or rarity) factor; they are prioritised and have extraordinary biodiversity and geodiversity features compared to other protected areas[2,3]. The UNESCO World Heritage Centre established a list of 14 primary factors of deterioration of the OUV ranging from human activities (development, pollution, social and cultural use), climate change and severe weather events, to invasive species, management and institutional factors[4]. Climate change and severe weather events can affect coastal areas through flooding, inundation and increased erosion[5–7]. 88 NWHS intersect the coast and include sites most at risk from climate change[8]. Although they have pristine environments, their coastlines are increasingly subject to anthropogenic pressures inside and outside their boundaries such as pollution, population growth, and development including port facilities, dams and pumping stations. Following the International Union for Conservation of Nature conservation Outlook assessment conducted in 2017[9], only 20% of coastal NWHS have a good conservation outlook, and the conservation of 39% of the sites is under significant to critical concerns. Moreover, the OUV of about two thirds of coastal NWHS are at high to very high threat from deteriorating factors. Additionally, these sites are subject to physical processes such as sea-level rise (SLR)[10–15] and human modifications to sediment budgets[16]. However, shoreline change is not systematically monitored or reported in many NWHS[17–19], so it is unclear how NWHS shorelines have or could change. As sites that have very limited internal anthropogenic disturbance, they present significant opportunities to analyse how and why shorelines change due to natural drivers and/or external pressures.

Previous assessments of shoreline change in heritage studies include local[20–23], regional[24] or global[25,26] studies. Local studies included the *Sundarbans* mangrove forests[21,23], the *Everglades National Park*[22], and the *Wadden Sea*[20]. A regional evaluation of 49 coastal Cultural World Heritage Sites around the coast of the Mediterranean found that 37 low-lying sites are at risk from a 100-year flood event today and that 42 sites are threatened by coastal erosion[24]. Two global studies have analysed the effects of future shoreline change due to SLR. The first determined that 80% of the coastal wetlands of international importance could be affected by a 0-1 m rise in sea level[27]. The second study found that 40 to 136 cultural and mixed coastal World Heritage Sites may be affected by flooding over 2 000 years if global temperatures and sea-levels continue to rise[25]. To date, no study has explored globally past multi-decadal shoreline change and its possible drivers in NWHS in term of their geomorphology, elevation, land cover, lithology, climate variability and sea-level change.

The availability of satellite images from 1984 to present via the Google Earth Engine has allowed the creation of a global consistent shoreline change dataset that can be used to monitor coastal NWHS[28–30]. In this paper, global datasets of shorelines, geomorphological conditions, and relevant forcing drivers are used to evaluate historic shoreline change from 1984 to 2016 across 67 coastal NWHS (out of 88 due to data availability limitations and data cleaning). The objectives are:

(1) To assess and classify historic shoreline change behaviour within the 67 coastal NWHS;
(2) To evaluate the geomorphological conditions associated with different shoreline behaviours (based on their linearity against time) and shoreline trends (recessional, depositional and stable); and
(3) To determine the impacts of historic sea-level change and climate variability on shoreline behaviour.

This paper is structured as follows. The data are introduced in Section 2. The methods and results are presented in Section 3 and Section 4 respectively. The discussion is presented in Section 5 and the conclusion in Section 6.

2 Data

Three datasets were used: (1) coastal NWHS sites boundaries and shoreline change time series (Section 2.1); (2) geomorphological datasets (Section 2.2); and (3) climate variability and sea-level change datasets (Section 2.3).

2.1 Study sites and shoreline change time series

Boundaries of coastal NWHS were retrieved from the World Database on Protected Areas[31]. 88 sites intersected the Global, Self-consistent, Hierarchical, High-resolution Shoreline database[32] (Figure 1). Shorelines were obtained from a global assessment of derived Landsat images[28–30]. This provided satellite-derived shorelines (SDS) data points and their yearly positions based on transects spaced 500 m apart. SDS data points were available for 71 out of 88 coastal NWHS due to limited coverage of historic satellite imagery in offshore waters. The raw shoreline time-series data were cleaned from transects containing less than five SDS data points and having a temporal coverage shorter than seven years[28]. Approximately 1.5 million time-series data points were selected. Further conditional and outlier data cleaning were undertaken (Supplementary Section A.1.1). The conditional cleaning was performed for more consistency on the assessment of shoreline trends: all transects that had at least 17 SDS data points were retained for the analysis (Supplementary Section A.1.1). The outliers' cleaning was performed to delete extreme SDS data points values (deviating by more than three times the standard deviation) within each transect (Supplementary Section A.1.1). The cleaning process (see flowchart in Supplementary Figure SM1) removed 3.8% of the raw SDS data points, and 67 sites remained in the analysis (Figure 1).

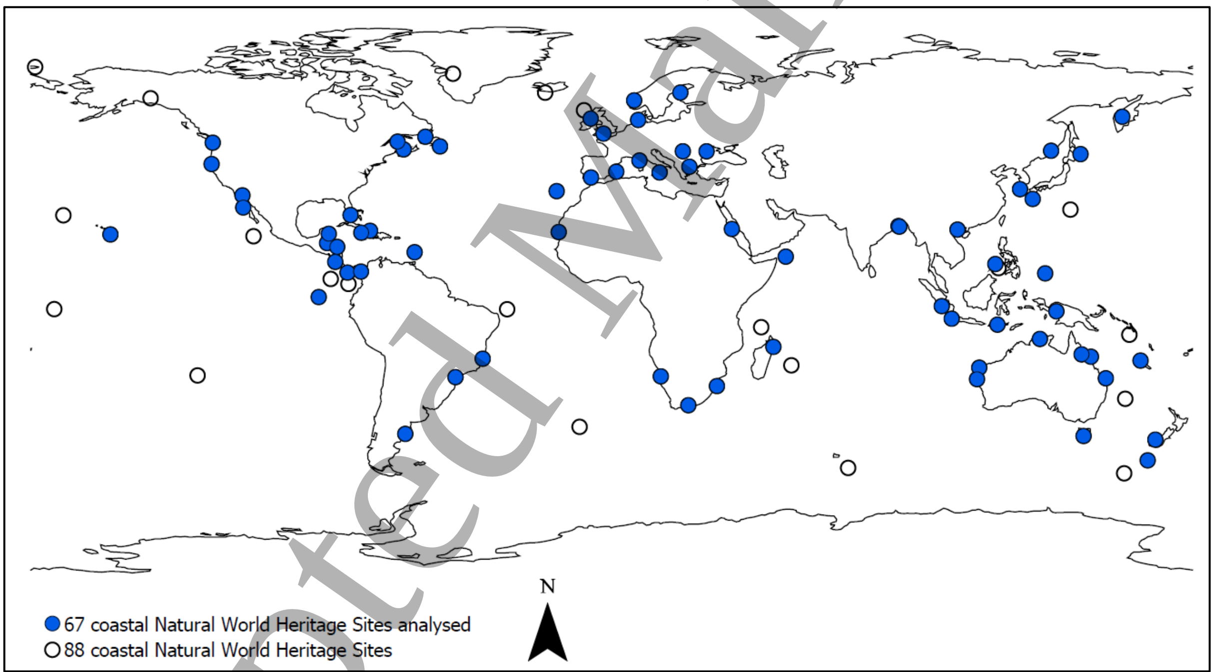

Figure 1 Geographical distribution of 88 coastal Natural World Heritage Sites around the world. 67 sites with available cleaned shoreline time-series data are analysed (Sources: World Database on Protected Areas[31], Global, Self-consistent, Hierarchical, High-resolution Shoreline database[32], and shoreline time-series data[28–30]).

2.2 Geomorphological conditions

Information of topography, land cover, coastal type and lithology (Table 1) was obtained from global databases to analyse how depositional and recessional shoreline change rates (SCR) varied (Supplementary Section A.1.2). The resolution of the topography and land covers datasets (~500 m at the equator) is similar to the shoreline data. The coastal type dataset resolution is 50 km and permits the classification of sites. The resolution of lithological data varies, starting from 5 m^2 and is adequate for both transect- and site-based analysis. These datasets are suitable due to their coverage of the study area allowing for a consistent analysis; moreover, their resolutions are suitable for a global and site-based assessment of shoreline trends.

Table 1 Summary data types, sources, resolutions and transects categorisation in terms of topography, land cover, coastal typology, and lithology. Details of data selection and classification are available in the Supplementary Section A.1.2.

Dataset	Source and Resolution	Categories
Topography (classification based on the distribution of the elevation of **strong linear transects)**	Global Map DEM (2017) [33] ~0.5km at the equator	1. 0 ≤ elevation ≤ 1 m (extremely low-lying) 2. 1 < elevation ≤ 10 m (low-lying) 3. 10 < elevation ≤ 50 m (middle) 4. 50 < elevation ≤ 400 m (high) 5. No data (transects without available elevation)
Land cover	Global Land Cover by National Mapping Organisations - GLCNMO (2013) [34] ~0.5km at the equator	1. Coral reefs 2. Mangroves 3. Marshes 4. Vegetated 5. Non-vegetated 6. Urban areas
Coastal type	Worldwide Typology of Nearshore Coastal Systems (2011) [35] Minimum resolution 50km	1. Small deltas 2. Tidal systems 3. Lagoons 4. Fjords and fjärds 5. Large rivers 6. Large rivers with tidal influence 7. Karst-dominated stretches of coasts 8. Arheic (dry areas) 9. Islands
Lithology	Global Lithological Map - GliM (2012) [36] Average resolution of 1:3 750 000 – polygons areas varies starting from 5 m^2	1. Evaporites 2. Polar ice and Glaciers 3. Acid Plutonic Rocks 4. Basic-Ultrabasic Plutonic Rocks 5. Intermediate Plutonic Rocks 6. Metamorphic Rocks 7. Carbonate Sedimentary Rocks 8. Mixed Sedimentary Rocks 9. Siliciclastic Sedimentary Rocks 10. Unconsolidated Sediments 11. Pyroclastic 12. Acid Volcanic Rocks 13. Basic Volcanic Rocks 14. Intermediate Volcanic Rocks

2.3 Climate variability and sea-level change

Between 1900 and 2016, global mean sea level has risen by 16-21 cm[37]. However, the effect of local SLR on the shoreline variability is poorly understood as often exceeded by climate variability, local geomorphological conditions, and/or human interventions[38]. Our study hypothesised that local trends of SLR[37] may have a potential observable contribution to strong linear shoreline trends within similar geomorphological categories in pristine NWHS sites, which should be negligibly affected by human interventions. To verify this hypothesis, local trends of sea-level change were assessed, and their effects on strong linear shoreline trends were determined within different geomorphological categories and sites. Linear available trends of local estimates of relative sea-level change[39] (measured by tide gauges) were used. These linear trends are appropriate as contemporary SLR acceleration rates are small (order of 0.1 mm^2 yr^{-1}) and are often not detectable at local tide gauge sites because of the large variability present in sea level[40]. Other driving forces of regional climate variability[41] (Table 2) were assessed as drivers of shoreline change. These yearly values of large-scale climate indices have been used in previous global assessments of surges and flooding[42,43] and have been shown to influence year-to-year variability in sea level[44–46]. The shoreline change dataset is 33 years of length, which is appropriate to capture the year-to-year variability that arises from climate forcing such as El Niño/Southern Oscillation (ENSO) or the other climate indices listed in Table 2.

Table 2 Regional climate variability indices description. The datasets are retrieved from https://psl.noaa.gov/data/climateindices/list/.

Index	Return periods	Description
El Niño/Southern Oscillation (ENSO) precipitation index	2 to 7 years[47,48]	Rainfall-based ENSO indices describing irregularly periodic variation in sea surface temperatures (SST) over the tropical eastern Pacific Ocean. The climate phenomenon periodically fluctuates between neutral, La Niña or El Niño[49].
Atlantic Multi-decadal Oscillation (AMO)	20 to 60 years[50,51]	SST anomalies occurring in the North Atlantic Ocean[52].
Arctic Oscillation (AO)	No particular periodicity[53]	Non-seasonal sea-level pressure (SLP) anomalies at the Arctic and Antarctic poles[54].
North Atlantic Oscillation (NAO)	No particular periodicity[55]	Atmospheric SLP between the Icelandic Low and the Azores High, which affects the westerly winds and location of storm tracks[56].
Niño 3, Niño 4 and Niño 3.4	2 to 7 years[47,48]	Indices used to monitor the tropical Pacific, all of which are based on SST anomalies averaged across a given region[57].
North Pacific (NP)	2 to 6 years or 7 to 12 years [58]	Area-weighted SLP over the region 30°N-65°N, 160°E-140°W[58].
Pacific Decadal Oscillation (PDO)	20 to 30 years[59]	Leading principal component of North Pacific monthly SST variability[60,61].
Southern Oscillation Index (SOI)	2 to 7 years[47,48]	Description of the development and intensity of El Niño or La Niña events in the Pacific Ocean (normalised index)[57].

3 Methods

Three stages of analysis were undertaken, corresponding to the three study objectives.

3.1 Shoreline change time-series: linear behaviour classifications and strong linear trends

Prior to fitting a linear regression, the potential linear behaviour of SDS data points, defined by their linearity against time, was assessed using Pearson's correlation coefficient (r) (R-3.5.1 package 'psych'[62]), with the statistical significance measured using the *p-value* (the closer r is to +/- 1 the stronger the linear relationship). Based on past qualitative description of r[63–65], shoreline change transects were divided as:

1. Strong linear (less than -0.7 or greater than 0.7);
2. Weak linear (-0.7 to -0.3 or 0.3 to 0.7); and
3. Non-linear (-0.3 to 0.3).

To assess the contributions of the three linear categories in the long-term shoreline change, mean annual SCR for the three linear categories were assessed using an Ordinary Least Square linear regression applied to transects based SDS[66]. The linear fit is a valid option to describe and forecast long-term predictive analysis and to minimise potential random error and short-time variability[66].

For the multi-decadal period considered in the analysis, linear regressions, which assume that the relationship between shoreline change and time is linear, are not relevant for shorelines changing with weak linear or non-linear behaviours. Thus, only SCR calculated for transects with strong linear shoreline behaviour are highly probable and significant on a multi-decadal scale and were selected to analyse depositional, recessional or stable SCR between 1984 and 2016. As the SDS accuracy is within a subpixel precision for the 33 years period analysed (15 m for Landsat), SCR between -0.5 and 0.5 m yr^{-1} were considered stable[28]. Depositional and recessional transects were defined by SCR >0.5 m yr^{-1} and <-0.5 m yr^{-1} respectively[28]. The mean and standard deviation of SCR were calculated for each geomorphological category and sub-category. Geomorphological categories and sub-categories with less than five transects were considered non-representative of mean shoreline change per category. Shoreline change outliers for strong linear transects were removed (<-21.16 m yr^{-1} for recessional transects and >23.05 m yr^{-1} for depositional transects) (see Supplementary Figures SM10 and SM11). 6 947 transects (98%) remained within 52 sites, after outliers were removed.

3.2 Geomorphological analysis

All transects were classified by their topography, land cover, coastal type and lithology (see Supplementary Section A.1.2). A comparison of the different geomorphological conditions for the strong linear, weak linear and non-linear shoreline behaviours has been conducted followed by an in-depth analysis of three transects' types of strong linear behaviour: recessional, depositional and stable.

3.3 Climate variability and sea-level change analysis

Comparisons of SDS data points per transect against a time series of climate indexes were undertaken using Kendall τ non-parametric rank correlation[43,67]. The comparison investigated potential dependencies between shoreline change and the ten climate indices defined in Section 2.3. The percentage of transects having a moderate/strong positive ($\tau>=0.5$) or moderate/strong negative ($\tau<= -0.5$) correlation with the time-series of climate indices was assessed for each category of transects defined by the Pearson's r classification. The contribution of sea-level change was assessed by fitting a linear regression between recessional and depositional strong linear SCR and local relative sea-level change for different land cover and coastal type categories. Additionally, a comparison between average shoreline evolution and relative sea-level change has been conducted for each site. Only shores with a mean elevation lower than 10 m (definition of the Low Elevation Coastal Zone[68]) were assessed.

4 Results

4.1 Classification of shoreline change time-series

The first objective was to assess and classify shoreline change linear behaviour in coastal NWHS between 1984 to 2016. All 67 sites had transects exhibiting at least two of the three linear shoreline behaviour categories (defined in Section 3.1). 52 of the 67 sites contained transects with strong linear shoreline behaviour. Across the 67 sites, data were available for 52 033 transects. 14% of these showed a significant strong linear behaviour at the 99.85% confidence level (Supplementary Table SM4). The percentage of transects with linear behaviour within each site varied from 0.2% (*Dorset and East Devon Coast*) to 63.5% (*The Sundarbans*) (Figure 2, Supplementary Table SM5). Under the hypothesis of long-term shoreline change, transects with strong linear behaviour had the highest mean recessional (-3.4 m yr^{-1}, std 3.6 m yr^{-1}) and depositional trends (3.5 m yr^{-1}, std 4.3 m yr^{-1}) in comparison to weak linear and non-linear shoreline categories (Supplementary Table SM6). The differences between strong linear, weak linear and non-linear shoreline behaviours with both depositional and recessional trends in relation to *r* are presented in Supplementary Table SM7 and Figures SM4 to SM9.

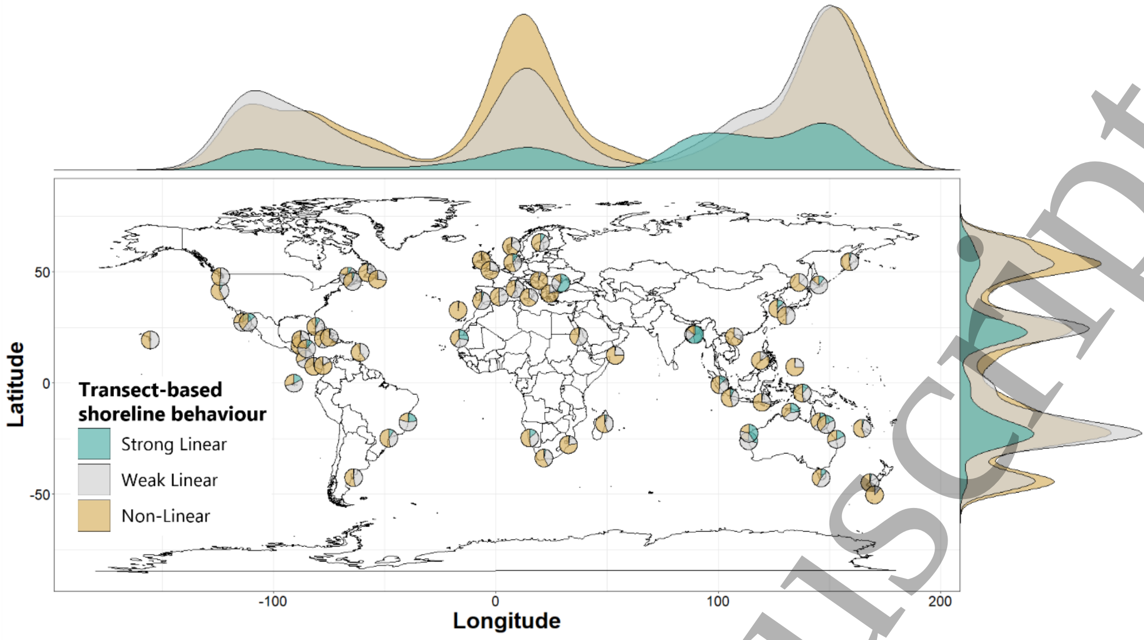

Figure 2 Globally distributed pie charts of strong linear, weak linear and non-linear transects (defined using Pearson's r coefficient) within the 67 coastal NWHS with available cleaned time-series shoreline data. The relative density plots show the relative distribution of each subset in relation to the complete dataset for the longitudes and the latitudes separately.

For the 7 087 transects in the 52 coastal NWHS showing strong linear shoreline behaviour, 52.8% had a recessional trend, 43% were accreting and 4.2% were stable. Among the sites with more than five remaining linear transects, *The Sundarbans (Bangladesh)*, *Danube Delta (Romania)*, and *Sundarbans National Park (India)* had the highest percentage of transects with a strong linear behaviour. The *Volcanoes of Kamchatka (Russia), The Sundarbans* and *Ujung Kulon National Park (Indonesia)* had the highest percentage of coasts with strong linear recessional shoreline change (97.6%, 84.9% and 84.6% were recessional of the total strong linear transects consecutively) (Figure 3). The *Banc d'Arguin National Park (Mauritania)*, *High Coast/Kvarken Archipelago (Sweden/Finland)*, and *Redwood National and State Parks (United States)* had the highest percentage with strong linear depositional shoreline change (98.3%, 91.1%, 90% are recessional of the total strong linear transects respectively) (Figure 3). Among all sites, *Río Plátano Biosphere Reserve (Honduras)* had the highest mean recessional SCR (-11.8 m yr^{-1}, std 7) and *The Wadden Sea (Netherland, Germany and Denmark)* had the highest mean depositional SCR (10.9 m yr^{-1}, std 5.7 m yr^{-1}) (Table 3).

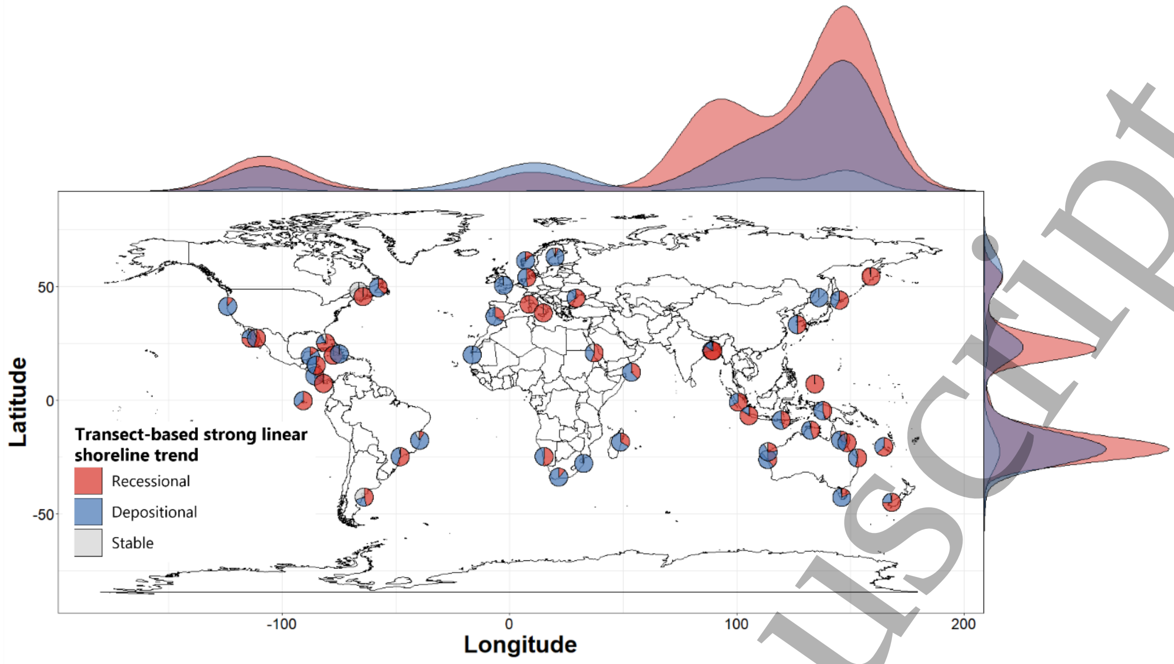

Figure 3 Globally distributed pie charts of recessional, depositional and stable shoreline trends within the 52 coastal NWHS with strong linear shoreline behaviour. The relative density plots show the relative distribution of each subset (recessional, depositional and stable) in relation to the complete dataset for the longitudes and the latitudes separately. Detailed percentages for each site are available in the Supplementary Table SM8.

Table 3 Number of transects, mean rates of change and standard deviations (std) for recessional, depositional and stable shoreline trend categories within a subset of coastal NWHS with the highest values of mean strong linear recessional and depositional trends. The sites, with more than five linear transects, are classified in descending order of the site-based mean rate of strong linear recessional shoreline change rates. A comprehensive assessment for all sites is available in the Supplementary Table SM9.

		Recessional shoreline change			Depositional shoreline change			Stable shoreline change		
Name	Coastline length (km)	Number of transects	Mean (m yr^{-1})	Std (m yr^{-1})	Number of transects	Mean (m yr^{-1})	Std (m yr^{-1})	Number of transects	Mean (m yr^{-1})	Std (m yr^{-1})
Río Plátano Biosphere Reserve	39	4	-11.8	7	4	2.7	2.8	0	0	0
Redwood National and State Parks	71	1	-9.3	0	9	3.7	2.1	0	0	0
Te Wahipounamu – South West New Zealand	1592.5	52	-8.6	6.7	21	1.8	0.7	2	-0.3	0.2
Socotra Archipelago	368	3	-7.8	0.9	5	5.4	1.5	0	0	0
The Wadden Sea	2 507.5	231	-7.5	4.6	240	10.9	5.7	0	0	0
Península Valdés	497	6	-7.2	5.4	3	0.7	0.2	4	0	0.4
Namib Sand Sea	359.5	46	-6.7	5	40	7.6	5.6	0	0	0
Atlantic Forest Southeast Reserves	382	41	-4.9	5.6	31	2.1	2.1	1	-0.4	0
The Sundarbans	503	528	-4.8	4	90	4.6	5.5	4	-0.4	0.1
Danube Delta	175.5	131	-4.6	2.9	66	4.6	4.9	0	0	0
Lorentz National Park	133.5	14	-4.3	4.7	16	6.6	4.8	0	0	0
Banc d'Arguin National Park	1 275	4	-1.8	1.3	227	6.1	3.9	0	0	0
iSimangaliso Wetland Park	66	0	0	0	10	4.9	1.2	0	0	0

4.2 Geomorphological analysis

The second objective was to evaluate the geomorphological conditions associated with different shoreline behaviours (based on their linearity against time) and shoreline trends (recessional, depositional and stable).

First, a comparison of the geomorphological compositions of strong linear, weak linear and non-linear shoreline behaviours was conducted (Figure 4). Transects with strong linear behaviour had a higher percentage of tidal systems (30%) and arheic systems (19%) while transects with non-linear and weak linear behaviours had a higher percentage of fjords/fjärds (14% and 9% consecutively) and islands (13% and 12% consecutively). Strong linear transects had a higher percentage of mangroves (40%) in comparison to non-linear and weak linear transects. Non-linear and weak linear transects had a higher percentage of different rock types (such as metamorphic, acid plutonic, basic plutonic, intermediate plutonic rocks) while transects with a strong linear behaviour had the highest percentage of unconsolidated sediments (74%). Transects with strong linear behaviour had a higher percentage of extremely low-lying (18%) and low-lying areas (61%).

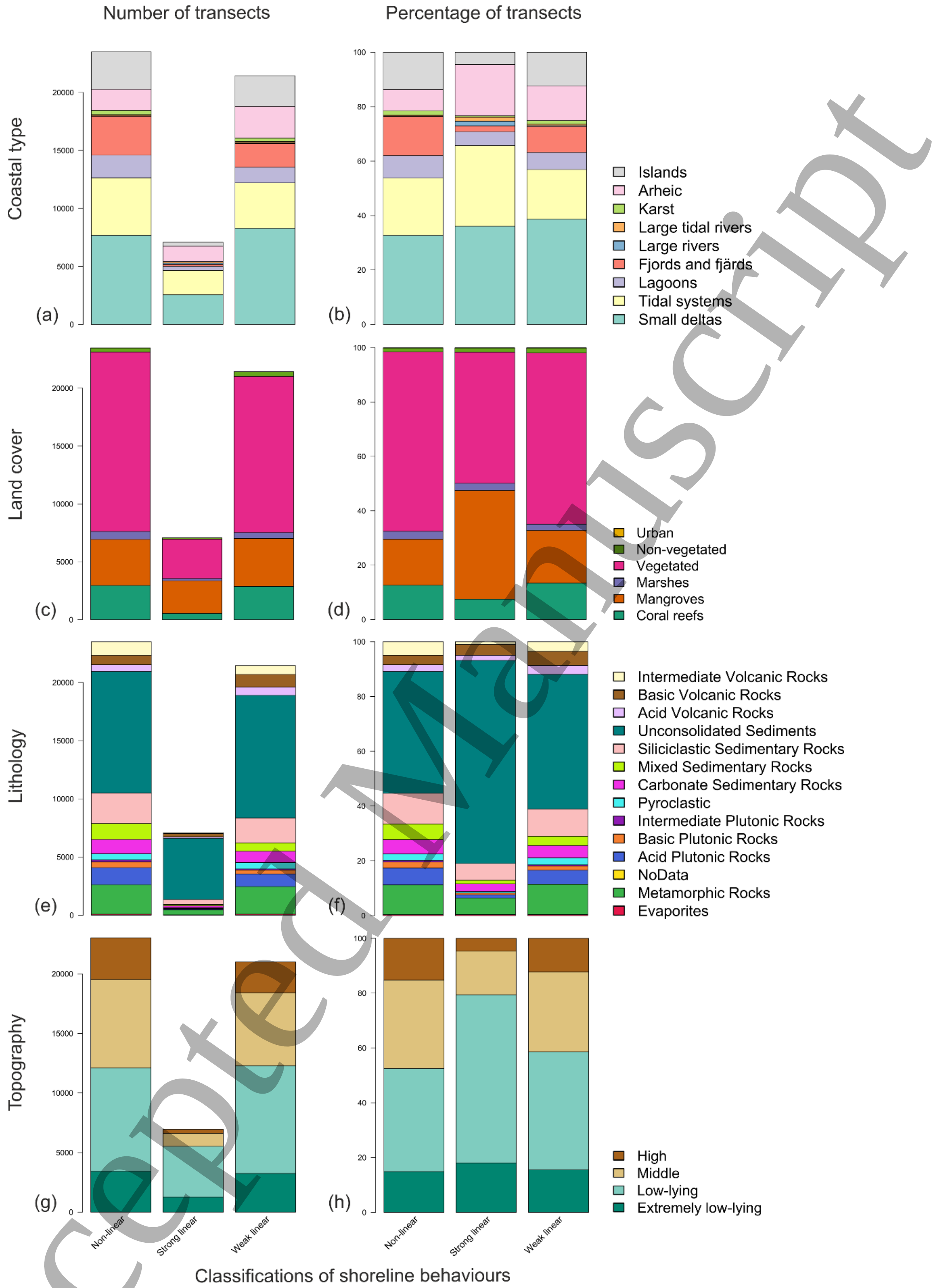

Figure 4 Number and percentage of transects for the three categories of shoreline behaviour: non-linear, weak linear and string linear classified by coastal type (a and b), land cover (c and d), lithology (e and f) and topography (g and h).

Second, the geomorphological conditions associated with strong linear recessional, depositional and stable shoreline trends are evaluated. For 297 stable transects in 18 sites, 62% of the transects had their mean elevation within [1-10 m] and 29% within [10-50 m]. Sable transects consisted of 42% small deltas, 31% arheic systems and 13% tidal systems (Figure 5). Within these coastal types, vegetated areas and mangroves were the prevailing land cover types (Figure 5). They represented respectively 53% and 34% of the totality of recessional transects. 71% of recessional transects were unconsolidated sediments, 6% siliciclastic sedimentary rock and 5% acid volcanic rocks. Further analysis were not conducted for stable strong linear shoreline trend as they represent only 4% of the totality of strong linear transects in 35% of the sites displaying a strong linear behaviour.

Within 3 664 recessional transects in 47 sites, 14% of the transects had their mean elevation within [0-1 m] and 68% within [1-10 m]. Recessional transects consisted of 36% tidal systems, 36% small deltas and 15% arheic systems (Figure 5). Within these coastal types, mangroves and vegetated areas were the prevailing land cover type (Figure 5). They represented respectively 52% and 38% of the totality of recessional transects. 81% of recessional transects were unconsolidated sediments, 6% siliciclastic sedimentary rock and 5% basic volcanic rocks. Within 2 986 depositional transects in 45 sites, 23% of the transects had their mean elevation within [0-1 m] and 51% within [1-10 m]. Depositional transects consisted of 36% small deltas, 23% tidal, and 23% arheic systems respectively (Figure 5). Within these coastal types, mangroves and vegetated areas were dominant (Figure 5). Vegetated areas, mangroves and coral reefs represented respectively 60%, 25% and 11% of the totality of accretive transects. 67% of accretive transects were unconsolidated sediments, 11% metamorphic rocks and 7% siliciclastic sedimentary rocks. The depositional trend decreased exponentially with increases in elevation (Supplementary Figure SM13). The highest depositional SCR were observed for transects with a mean elevation lower than 1 m (Table 4).

Among all elevations categories, the comparison of land cover categories shows that transects within the elevation category [0-1 m] with vegetated areas had the highest mean rate of shoreline recession (-5.9 m yr^{-1}, std 4.3 m yr^{-1}) (Table 4). Transects within a 1 km geodesic distance from coral reefs had the lowest recessional trend (mean -1.7 m yr^{-1}, std 1.8 m yr^{-1}). For elevations <1m, among all geomorphological categories, the highest mean rates of recession (-8.1 m yr^{-1}, std 5.2 m yr^{-1}) was observed in transects composed of unconsolidated sediment within the category of vegetated tidal systems in the *Wadden Sea* (Supplementary Table SM10). For low-lying areas, the highest mean recession of -8.9 m yr^{-1} (std 4.2 m yr^{-1}) was observed in transects composed of siliciclastic sedimentary rocks within the category of vegetated tidal systems (Supplementary Table SM11). For the middle-elevation category, the highest mean shoreline recessive trend was observed within metamorphic rock transects situated in vegetated fjords (-7.5 m yr^{-1}, std 7.2 m yr^{-1}) in *Te Wahipounamu (New Zealand)* (Supplementary Table SM12). For the high-elevation category, the greatest mean recession was in metamorphic rock transects in vegetated fjords and fjärds situated in *Te Wahipounamu* and *West Norwegian Fjords (Norway)* (-13.1 m yr^{-1}, std 6.2 m yr^{-1}) (Supplementary Table SM13).

For all topographic categories, extremely low-elevation transects within vegetated areas had the highest mean accretive trend (7.0 m yr^{-1}, std 5.8 m yr^{-1}) (Table 4). Transects within a 1 km geodesic distance from coral reefs had the lowest accretive trend (Table 4). Within extremely low-elevated transects, the highest mean accretive trends were observed in transects composed of vegetated tidal systems (12.5 m yr^{-1}, std 5.4 m yr^{-1}, in the *Wadden Sea*) and vegetated large rivers within a tidal delta (11.0 m yr^{-1}, std 5m yr^{-1}, in the *Islands and Protected Areas of the Gulf of California (Mexico)*) (Supplementary Table SM14). Within low-elevated transects, the highest mean depositional trend of 13.6 m yr^{-1} (std. 5.3 m yr^{-1}) was observed in transects composed of evaporites within the category of vegetated small deltas situated within the *Namib Sand Sea (Namibia)* (Supplementary Table SM15). For the middle-elevation category, the highest accretive trend was observed within transects situated in tidal coastal systems covered by mangroves (4.6 m yr^{-1}, std 5.4 m yr^{-1}) (Supplementary Table SM16). Coastal ecosystems with this shoreline trend were found in *Kakadu National Park*, *Lorentz National Park* and *The Sundarbans*. For high elevation transects, the greatest mean accretive shoreline change was found in tidal systems with mixed sedimentary rocks in *Tasmanian Wilderness* (4.4 m yr^{-1}, std 6 m yr^{-1}) (Supplementary Table SM17).

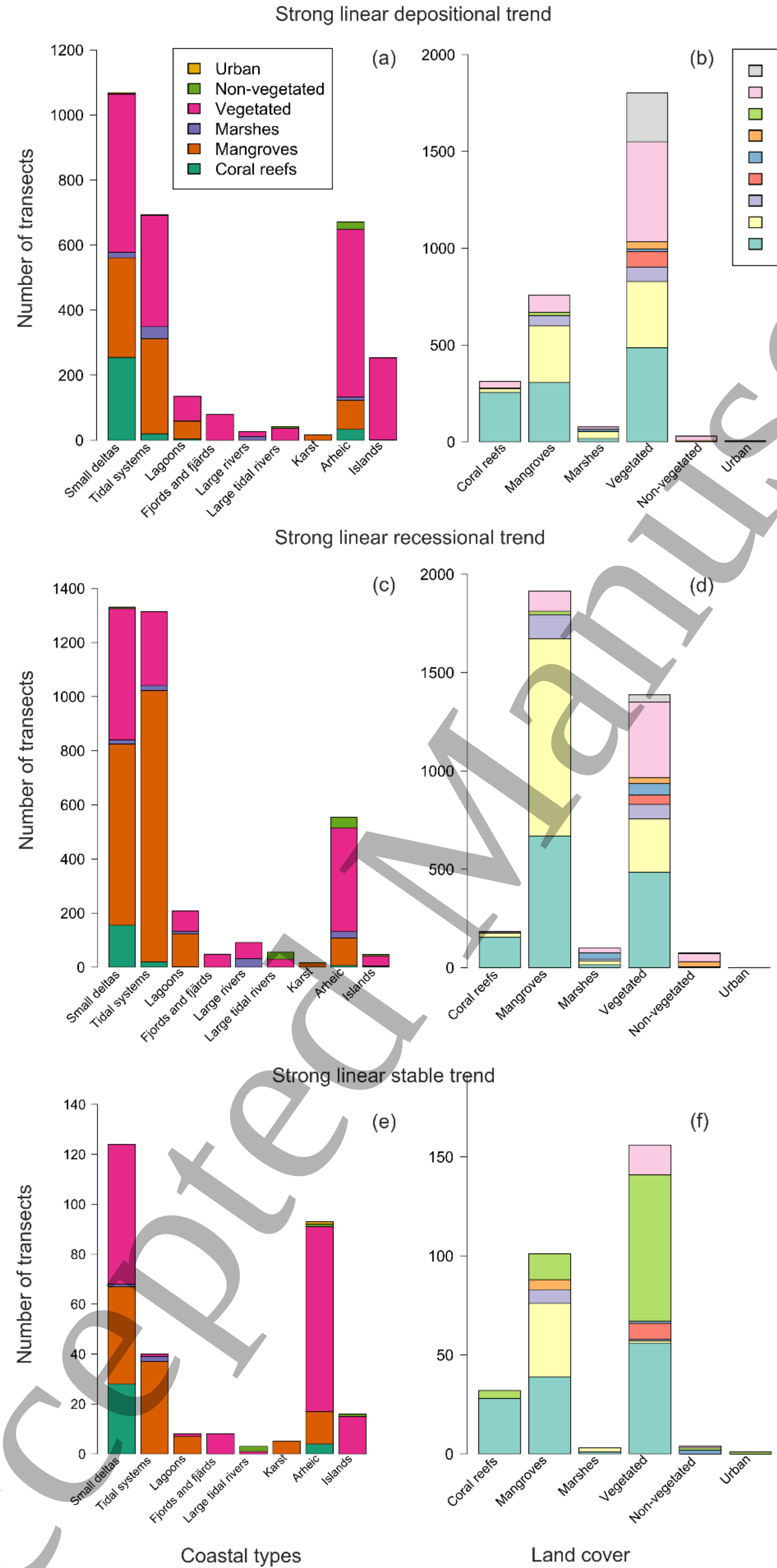

Figure 5 Number of transects with a strong linear depositional (a and b), recessional (c and d) and stable (e and f) shoreline trends within the categories of coastal types and land covers: coastal types are classified in term of land covers and land covers are classified in term of their coastal type conversely.

Table 4 Mean strong linear recessional and depositional shoreline change rates (m yr^{-1}) within the elevation categories and corresponding land cover sub-categories. Grey cells correspond to non-representative or non-existent categories. Categories with less than ≤ 5 transects are considered as non-representative of the shoreline change within each category. Detailed results for other geomorphological categories and subcategories are available in the Supplementary Sections A.2.3 and A.2.4.

Mean strong linear recessional and depositional shoreline trends for topographical and land cover categories (m yr^{-1})

Topographical categories			**Coral reefs**		**Mangroves**		**Marshes**		**Vegetated**		**Non-vegetated**		**Urban**	
0 ≤ elevation ≤ 1 m	-5.3	6.7	-1	1	-3	3.7	-4.7	5.9	-5.9	7	-3.8	4.3		
1 < elevation ≤ 10 m	-3.1	2.7	-1.5	1.6	-3.2	2.7	-3.1	2.9	-3.1	3.1	-3.3	2.4	-1.2	1.7
10 < elevation ≤ 50 m	-2.3	2	-1.9	1.8	-2.4	2.5		1.7	-2.4	2	-1.7	1.2		
50 < elevation ≤ 400 m	-5.1	1.4	-1.2	1					-5.5	1.5				

4.3 Climate variability and sea-level change analysis

The third objective was to determine the impacts of historic sea-level change and climate variability on shoreline behaviour in coastal NWHS. The comparison of yearly transect-based time series of shorelines (within the three categories of linear shoreline change behaviour) against ten climate indices indicated no significant statistical association at global scale (Supplementary Table SM18). Globally and for different geomorphological categories and sub-categories, there was no positive correlation between shoreline change and relative sea-level change for transects with strong linear recessional or depositional trend. Thus the absolute value of recessional SCR did not increase and the value of depositional SCR did not decrease with increasing relative sea-level change values for low lying transects (0 to 10 m) (Figure 6 and Supplementary Figure SM14). A weak positive relationship was observed between recessional strong linear shoreline trend and relative sea-level change in vegetated tidal systems below 1 m in the *Wadden Sea* (Figure 7). No correlation has been found between the average shoreline change rate and the average relative SLR for each site (Supplementary Figure SM15).

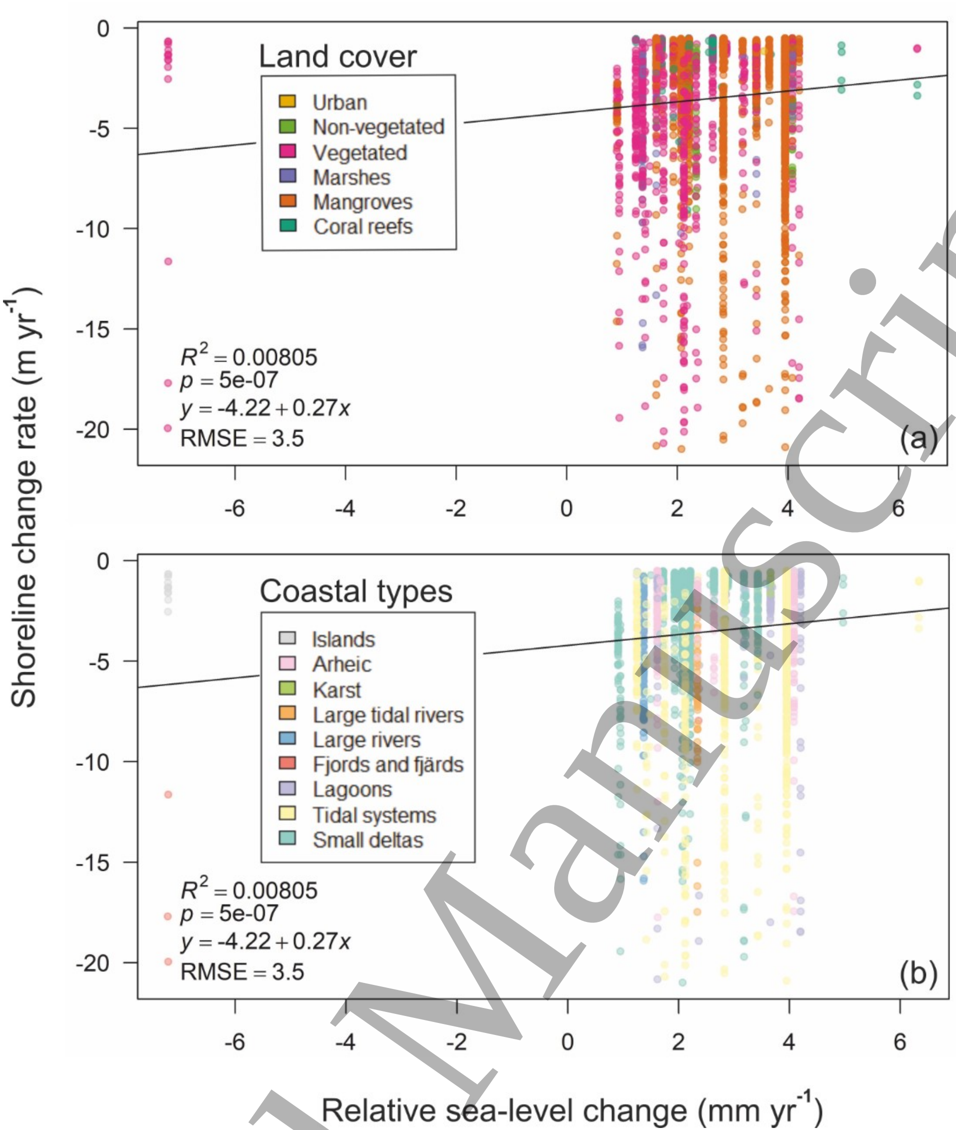

Figure 6 Correlation between recessional shoreline change rates and relative sea-level change for low lying transects (0 to 10 m) with a strong linear behaviour. The categorisation of transects is based on their land cover (a) and coastal type (b). The results for strong linear depositional shoreline trends are available in Supplementary Figure SM14.

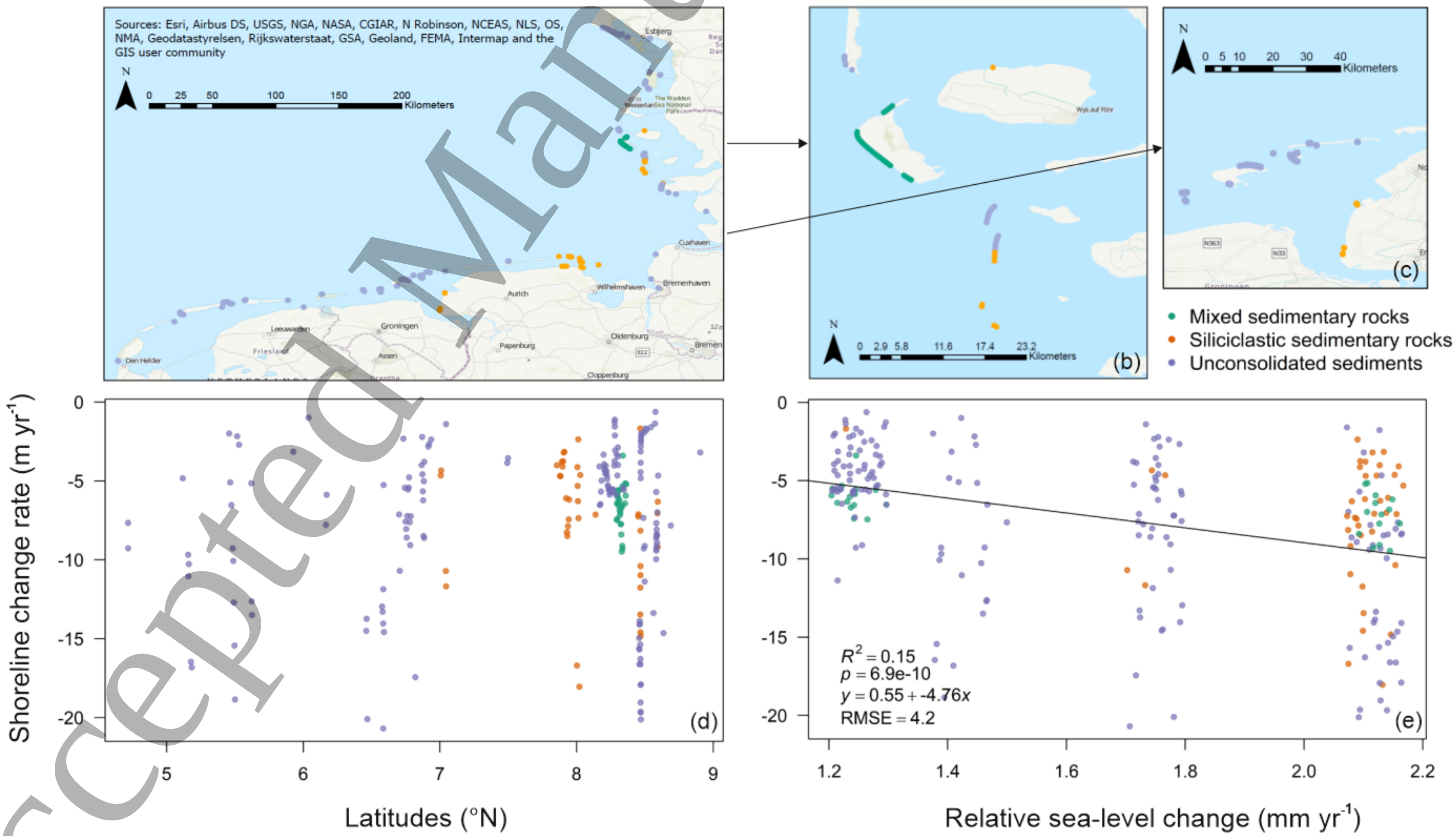

Figure 7 (a), (b) and (c) Maps of strong linear recessional shoreline change positions for transects below 1 m in the *Wadden Sea* vegetated tidal systems. (d) Latitudinal distribution of shoreline change. (e) Correlation between strong linear recessional shoreline change rates and relative sea-level change. The categorisation of transects is based on their lithological categorisation.

5 Discussion

This paper has presented the first global assessment of trends and drivers of shoreline change in coastal Natural World Heritage sites from 1984 to 2016. The data showed that both extreme erosional and accretional tendencies were apparent and one tendency did not dominate in these sites. A classification of linear behaviour with time indicated that strong linear shoreline trends have a significant contribution to the recessional (-3.4 m yr^{-1}, std 3.6 m yr^{-1}) and depositional trends (3.5 m yr^{-1}, std 4.3 m yr^{-1}). The prevalence of unconsolidated sediment in transects with strong linear behaviour demonstrates the potential contribution of coastal sediment processes (affected by human disturbances, waves, tides and tidal currents, wind, currents and sea-level change).

Drivers of strong linear recessional and depositional trends were assessed using geomorphological categorisation of transects, including analysis of case studies (Supplementary A.3 Discussion). Low lying transects had the highest mean depositional and recessional linear shoreline trends with (6.7 m yr^{-1} and -5.3 m yr^{-1}) for transects in [0-1 m] and (2.7 m yr^{-1} and -3.1 m yr^{-1}) for transects in [1-10 m]. This is partly explained by the lithological compositions of these low-lying environments and the presence of lagoons, sandy beaches, large rivers and large rivers under tidal influences. *Río Plátano Biosphere Reserve* has the highest mean shoreline recession (-11.8 m yr^{-1}, std 7.01 m yr^{-1}) due to the 2002 opening of an inlet 12 km northwest of Iban lagoon inducing new accretive and erosive processes within the site boundaries that are influenced by Paulaya river sediment discharge and the southeast-northwest ocean current from Honduras to Yucatan[69]. Sediment deposition, shaped by the Benguela Upwelling system, southwest of the *Namib Sand Sea*'s Conception Bay (evaporite basin) and Sandwich harbour had induced the highest mean accretive shoreline of all coastal NWHS (13.6 m yr^{-1}, std 5.3 m yr^{-1})[70]. Transects with high mean rates of change (10.1 m yr^{-1} and -7 m yr^{-1}) were found in large rivers within tidal delta situated in the vegetated shorelines of *Islands and Protected Areas of the Gulf of California.* This extreme trend is linked to natural forcing (wave and tides) but also to the decadal legacy of distant human alterations that interrupts completely constructive processes within the delta and creates new hydrological circulations accompanied by "unnatural" erosive/accretive processes[71–73]. High sedimentary movements, found in vegetated shores (6.9 m yr^{-1} and -5.1 m yr^{-1}) and marshes (5.4 m yr^{-1} and -5.7 m yr^{-1}) in large river systems are due to the construction of engineered structures along the rivers and on the coasts. These extreme rates are observed in the *Danube Delta* that underwent a large decrease in its sediment discharge due to up-stream damming projects (1970 and 1983) in parallel to the undesirable effects of extreme downdrift erosion southward of Sulina Jetties engineered in the second half of the 19th century[74–77]. Extreme rates of changes are also observed within vegetated tidal systems (8.2 m yr^{-1} and -6.8 m yr^{-1}) and more specifically within barrier islands in the *Wadden Sea*. The largest unbroken system of intertidal sand and mudflats in the world is a result of dramatic morphodynamic adjustments due to land reclamation (at the boundaries of the NWHS) within the climatic environment of the Frisian coast, which supported the reduction of inlet width (and tidal prism) and thus the growth of the islands[78,79]. The mainland and some islands of *the Wadden Sea* are engineered (sand nourishment, breakwaters dykes, and dunes protection) and accretive transects are prevalent (Supplementary Figure SM19)[80–84]. Thus, both depositional and recessional large shoreline trends in coastal NWHS can be linked to coastlines that are highly altered by human intervention external and internal to a site's boundaries.

Transects within small deltas and arheic systems inside 1 km geodesic buffer from coral reefs have the lowest accretive and recessional shoreline trend ((1.5 m yr^{-1} and -1.5 m yr^{-1}) and (1.7 m yr^{-1} and -0.9 m yr^{-1}) respectively). This trend may be explained as coral reefs provide sediments and coastal protection from waves, storms and floods and minimise the effects of coastal processes on the coastlines[85–87]. Most of the sites with coral reefs (such as the *Great Barrier Reef (Australia)*, *Shark Bay (Australia)*, and *Komodo National Park (Indonesia)*) are under frequent bleaching events in recent years (for instance the third bleaching event 2014-2017 was among the worst ever observed)[88,89]. Unconsolidated sediments within tidal systems protected by coral reefs show less stability than non-tidal systems with higher rates of erosion (-3.4 m/y; std 1 m/y) and accretion (2.1 m/y; std 1.5m/y) in the *Great Barrier Reef* and *Lagoons of New Caledonia: Reef Diversity and Associated Ecosystems*. The reef systems within the latter coastal NWHS are among the most affected by present and projected future bleaching events[88]. Coral reefs also deteriorate through overfishing, sewage and agriculture pollution and invasive species[90,91]. Further deterioration of coral reefs would weaken their function to maintain stable coastlines, especially beaches[87,88].

While the shoreline change dataset describes well the changes for continental unconsolidated sediments or sedimentary rocks, it does not demonstrate well shoreline change for coastal transects situated within complex narrow bodies of water as fjords (such as *Te Wahipounamu*, and the *West Norwegian Fjords*) or remote rocky cliffs (such as the *Galapagos Islands*). A visual verification using Google Time-lapse does not show the extreme linear shoreline trend captured by the SDS for these natural systems and informs on the limitation of shoreline detection methodology using satellite images. These errors may occur during (1) image detection: geometric distortion and radiometric errors[92] or (2) image processing: geo-rectification, ortho-rectification[93] and shoreline extraction.

Overall, there are no statistically significant correlations between transect-based shoreline change and the climatic indices of sea surface temperature and pressure anomalies. This may be explained by the limited spatial and temporal resolution of the climatic data and the underlying satellites images used to assess shoreline trends. In Low Elevation Coastal Zones, the analysis of shoreline trends demonstrate that no major historic role of relative sea-level change in accretional or recessional shoreline trend can be identified. One issue is that SLR shows limited variability in time and space over the study period. Further, the high variability at many sites emphasises that other processes, in addition to SLR, are operating. This may be due to different responses of sites to sea-level change, the lack of observations on coastal dynamics and their driving processes and that even in rapidly subsiding coasts other processes (i.e. storms, wave action, human activities) may dominate the shoreline trend[38,94]. However, for transects below 1 m in the vegetated tidal sedimentary systems and marshes of the *Wadden Sea*, a weak correlation between increasing relative sea-level and shoreline strong linear retreat was detected. This may be explained by rising sea-levels resulting in more inundation but also coastal erosion in low-lying areas[95,96]. The detection of this weak correlation may be related to the better quality of tide gauge data available in the *Wadden Sea* and to the site's highly dynamic tidally influenced inlets that experience one of the highest mean recession (-8.1 m yr^{-1}, std 5.2 m yr^{-1}) in NWHS worldwide[78,97]. This finding is supported due to the accuracy of shoreline detection methods (0.5 m yr^{-1}) allowing observation of increased shoreline change as a result of SLR. For instance, following the Bruun rule[98], 1 mm yr^{-1} of SLR could induce at least an incremental horizontal change of 1.65 m in a beach slope of 1:50 over 33 years. Detection of climate variability and sea-level change effects on shoreline behaviour could be improved by using higher satellites image resolution (e.g. 1m), developing monthly time-series of shoreline change (instead of annual time-series) and improving the spatial and temporal resolution of sea level and climatic data especially in remote areas.

The intensification of human interferences, climate change, SLR and wave climate change will affect coastal processes inducing variations in sediment-budgets[99]. Future SLR may become the main driver of recession[99] effecting geomorphological responses. Eroding low-lying shorelines within tidal systems, large rivers and large rivers under tidal influences, altered by human interferences to coastal processes, may become the most affected coastal NWHS by future SLR and its related changes in sediment dynamics. In the *Wadden Sea* while contemporary slow sea-level change has expressed itself in losses of beaches or island displacements[100–102], future acceleration of SLR may induce back-barrier erosion and sediment deficit in the tidal basin and result in the transformation of the inter-tidal system to a lagoon system[20,103]. The mapping of shoreline linear behaviour and depositional/recessional trends distinguishing abrupt and gradual changes at the transect level, coupled with socio-economic and ecologic indicators, can be used by coastal managers as a preliminary classification of shorelines in term of the importance and urgency of their management, supporting NWHS conservation triage (process of prioritising actions)[104,105]. The enhanced predictive capacity of strong linear shoreline behaviour and the improved understanding of the factors causing this strong linear changes need to be followed by more appropriate management actions, monitoring and planning of coastal NWHS sites' evolving shorelines (when required and to the extent possible). Unconsolidated sediment shorelines in coastal NWHS, not affected by external human interferences, which exhibit a strong linear behaviour of shoreline change, may become primary observatories to assess SLR impacts on natural coastal processes such as in *Río Plátano Biosphere Reserve* and the *Namib Sea*. Thus, this study contributes to informing coastal management plans and decisions of coastal and marine protected areas by providing a quantitative evaluation of shoreline behaviour that could improve the guide for Planners and Managers for Marine and Coastal Protected Areas (developed by Salm & Clark [106]).

6 Conclusions

Despite the high local and international values of coastal NWHS, shoreline change has not been systematically monitored or reported to date. Therefore, it was unclear how NWHS coasts have been changing across the world. This study comprises the first global assessment of multi-decadal shoreline change from 1984 to 2016 within coastal NWHS asking: "how are coastal NWHS shorelines changing around the world and why?".

Based on newly available open-access datasets, shoreline change was analysed for 67 NWHS worldwide, in terms of linear behaviour, recessional or accretive trends, and potential drivers of change. Shorelines with strong linear erosional or accretive trends comprise 14% of total coastal NWHS shorelines. They occur within 52 coastal NWHS and demonstrate the largest shoreline erosive and accretive trends (mean of -3.4 m yr^{-1} and 3.5 m yr^{-1}, respectively). Among the transects with strong linear behaviour, the highest recessional and accretive trends are found within low-lying unconsolidated sediments shorelines (< 1m) in vegetated tidal coastal systems, and vegetated tidal deltas at the mouth of large river systems. These extreme shoreline trends can be linked to natural coastal morphodynamics such as the opening of inlets or gradient of alongshore sediment transport. In other cases, they can be associated with direct or indirect human interferences such as land reclamation and damming of rivers upstream of a delta. Conversely, the most stable soft coasts are associated with shorelines protected by coral reefs ecosystems. In the future, these shorelines may be subject to increased instability due to the intensification of climate change and human deterioration degrading the natural protective capacity of coral reefs. A positive correlation between recessional (strong linear) shoreline change and relative sea-level change was found in the *Wadden Sea*, but globally, the effects of SLR on shoreline change are not apparent.

In most cases, shoreline monitoring had not been the main priority in the management of coastal NWHS. The availability of open-access datasets creates opportunities to better understand shoreline change so to inform management actions where necessary. These analyses can be repeated and refined providing new insights, as data extend in time and improve in resolution. Continued systematic monitoring is advised, especially for sites undergoing direct or indirect human interference.

7 Acknowledgements

We acknowledge the researchers at Deltares for their support throughout this project. We thank all the researchers who have made their global datasets available. Salma Sabour received funding via the Leverhulme Trust Doctoral Training Scheme, hosted by Southampton Marine and Maritime Institute at the University of Southampton.

8 Data availability statement

The data that support the findings of this study are openly available at http://doi.org/10.5281/zenodo.3751980.

Interactive maps based on the linear classification and on the strong linear trends of coastal NWHS transects are available at https://salmasabour.github.io/shoreline-change-coastal-natural-heritage-UNESCO/shoreline-linear-behaviours/ and https://salmasabour.github.io/shoreline-change-coastal-natural-heritage-UNESCO/shoreline-strong-linear-trends/ respectively.

9 Bibliography

1. UNESCO. *Operational Guidelines for the Implementation of the World Heritage Convention*. https://whc.unesco.org/en/guidelines/ (2017).
2. Le Saout, S. *et al.* Protected areas and effective biodiversity conservation. Supplementary Material. *Science (80-.).* **342**, 803–5 (2013).
3. Bertzky, B. *et al. Terrestrial Biodiversity and the World Heritage List*. https://portals.iucn.org/library/sites/library/files/documents/2013-016.pdf (2014).
4. UNESCO WHC. UNESCO World Heritage Centre - List of factors affecting the properties. http://whc.unesco.org/en/factors/ (2008).
5. Dawson, R. J. *et al.* Integrated analysis of risks of coastal flooding and cliff erosion under scenarios of long term change. *Clim. Change* **95**, 249–288 (2009).
6. Sweet, W. V *et al.* Global and Regional Sea Level Rise Scenarios for the United States. 1–75 (2017).
7. Rasmussen, D. J. *et al.* Extreme sea level implications of 1.5 °C, 2.0 °C, and 2.5 °C temperature stabilization targets in the 21st and 22nd centuries. *Environ. Res. Lett.* **13**, 034040 (2018).
8. Perry, J. World Heritage hot spots: A global model identifies the 16 natural heritage properties on the World Heritage List most at risk from climate change. *Int. J. Herit. Stud.* **17**, 426–441 (2011).
9. IUCN. *A conservation assessment of all natural World Heritage sites*. (2017). doi:10.2305/IUCN.CH.2017.17.en.
10. Nicholls, R. J. Impacts of and Responses to Sea-Level Rise. in *Understanding Sea-Level Rise and Variability* 17–51 (2010). doi:10.1002/9781444323276.ch2.
11. Vitousek, S. *et al.* Doubling of coastal flooding frequency within decades due to sea-level rise. *Sci. Rep.* **7**, 1399 (2017).
12. Church *et al.* Sea-Level Rise by 2100. *Science (80-.).* **342**, 1445–1445 (2013).
13. Gregory, J. Projections of Sea Level Rise. *IPCC Fifth Assess. Rep.* 16 (2013).
14. Goodwin, P., Haigh, I. D., Rohling, E. J. & Slangen, A. A new approach to projecting 21 st century sea-level changes and extremes. *Earth's Futur.* (2017) doi:10.1002/2016EF000508.
15. Brown, S. *et al.* Quantifying Land and People Exposed to Sea-Level Rise with No Mitigation and 1.5 and 2.0 °C Rise in Global Temperatures to Year 2300. *Earth's Futur.* (2018) doi:10.1002/2017EF000738.
16. Dunn, F. E. *et al.* Projections of declining fluvial sediment delivery to major deltas worldwide in response to climate change and anthropogenic stress. *Environ. Res. Lett.* **14**, (2019).
17. IUCN. *IUCN World Heritage Outlook*. (2017).
18. IUCN. IUCN Conservation Outlook Assessments - Guidelines for their application to natural World Heritage Sites. **2**, 1–35 (2012).
19. UNESCO. Climate Change and World Heritage: Report on predicting and managing the impacts of climate change on World Heritage and strategy to assist State Parties to implement appropriate management responses. *World Herit. Reports* **22**, 1–55 (2007).
20. Trilateral Working Group on Coastal Protection and Sea Level Rise. Final Report of the Trilateral Working Group on Coastal Protection and Sea Level Rise. *Wadden Sea Ecosyst.* **13**, 64 (2001).
21. Pahlowan, E. U. & Hossain, A. T. M. S. A disparity between erosional hazard and accretion of the sundarbans with its adjacent east coast, Bangladesh: a remote sensing and GIS approach. in *Volume 9644 SPIE Remote Sensing* 96441G (2015). doi:10.1117/12.2196386.
22. Park, J., Stabenau, E., Redwine, J. & Kotun, K. South Florida's Encroachment of the Sea and Environmental Transformation over the 21st Century. *J. Mar. Sci. Eng.* **5**, 31 (2017).
23. Loucks, C., Barber-Meyer, S., Hossain, A. A., Barlow, A. & Chowdhury, R. M. Sea level rise and tigers: Predicted impacts to Bangladesh's Sundarbans mangroves. *Clim. Change* **98**, 291–298 (2009).
24. Reimann, L., Vafeidis, A. T., Brown, S., Hinkel, J. & Tol, R. S. J. Mediterranean UNESCO World

Heritage at risk from coastal flooding and erosion due to sea-level rise. *Nat. Commun.* **9**, (2018).

25. Marzeion, B. & Levermann, A. Loss of cultural world heritage and currently inhabited places to sea-level rise. *Environ. Res. Lett.* **9**, 034001 (2014).
26. Sherbinin, A. de & Lacko, A. Evaluating the risk to Ramsar Sites from climate change induced sea level rise. *Ramsar Sci. Tech. Brief. Note* **5**, (2012).
27. Sherbinin, A. de, Lacko, A., Alexander, S. & Rep-, S. Evaluating the risk to Ramsar Sites from climate change induced sea level rise. *Ramsar Sci. Tech. Brief. Note* **5**, (2012).
28. Luijendijk, A. *et al.* The State of the World's Beaches. *Sci. Rep.* **8**, 1–11 (2018).
29. Hagenaars, G., de Vries, S., Luijendijk, A. P., de Boer, W. P. & Reniers, A. J. H. M. On the accuracy of automated shoreline detection derived from satellite imagery: A case study of the sand motor mega-scale nourishment. *Coast. Eng.* **133**, 113–125 (2018).
30. Hagenaars, G., Luijendijk, A., De Vries, S. & De Boer, W. Long term coastline monitoring derived from satellite imagery. in *Coastal Dynamics* 1551–1562 (2017).
31. IUCN. Protected Planet. *Database* 1–9 https://www.protectedplanet.net/ (2010).
32. Wessel, P. & Smith, W. H. F. A global, self-consistent, hierarchical, high-resolution shoreline database. *J. Geophys. Res. Solid Earth* **101**, 8741–8743 (1996).
33. International Steering Committee for Global Mapping. Global Map data archives. https://globalmaps.github.io/.
34. Kobayashi, T. *et al.* Production of Global Land Cover Data – GLCNMO2013. *J. Geogr. Geol.* **9**, 1 (2017).
35. Dürr, H. H. *et al.* Worldwide Typology of Nearshore Coastal Systems: Defining the Estuarine Filter of River Inputs to the Oceans. *Estuaries and Coasts* **34**, 441–458 (2011).
36. Hartmann, J. & Moosdorf, N. The new global lithological map database GLiM: A representation of rock properties at the Earth surface. *Geochemistry, Geophys. Geosystems* **13**, 1–37 (2012).
37. Church, J. a. *et al.* Sea level change. *Clim. Chang. 2013 Phys. Sci. Basis. Contrib. Work. Gr. I to Fifth Assess. Rep. Intergov. Panel Clim. Chang.* 1137–1216 (2013) doi:10.1017/CB09781107415315.026.
38. Le Cozannet, G., Garcin, M., Yates, M., Idier, D. & Meyssignac, B. Approaches to evaluate the recent impacts of sea-level rise on shoreline changes. *Earth-Science Reviews* vol. 138 47–60 (2014).
39. NOAA. Sea Level Trends. *Tides Curr.* 2012 (2012).
40. Haigh, I. D. *et al.* Timescales for detecting a significant acceleration in sea level rise. *Nat. Commun.* **5**, 1–11 (2014).
41. NOAA. ESRL : PSD : Climate Indices: Monthly Atmospheric and Ocean Time Series. https://www.esrl.noaa.gov/psd/data/climateindices/list/.
42. Mawdsley, R. J. & Haigh, I. D. Spatial and Temporal Variability and Long-Term Trends in Skew Surges Globally. *Front. Mar. Sci.* **3**, 1–17 (2016).
43. Muis, S., Haigh, I. D., Guimarães Nobre, G., Aerts, J. C. J. H. & Ward, P. J. Influence of El Niño-Southern Oscillation on Global Coastal Flooding. *Earth's Futur.* **6**, 1311–1322 (2018).
44. White, N. J. *et al.* Australian sea levels-Trends, regional variability and influencing factors. *Earth-Science Rev.* **136**, 155–174 (2014).
45. McCarthy, G. D., Haigh, I. D., Hirschi, J. J. M., Grist, J. P. & Smeed, D. A. Ocean impact on decadal Atlantic climate variability revealed by sea-level observations. *Nature* **521**, 508–510 (2015).
46. Amiruddin, A. M., Haigh, I. D., Tsimplis, M. N., Calafat, F. M. & Dangendorf, S. The seasonal cycle and variability of sea level in the South China Sea. *J. Geophys. Res. Ocean.* **120**, 5490–5513 (2015).
47. NOAA. Climate Prediction Center - ENSO Cycle. https://www.cpc.ncep.noaa.gov/products/analysis_monitoring/ensocycle/ensocycle.shtml.
48. NOAA. El Nino/Southern Oscillation (ENSO) | Teleconnections | National Centers for Environmental Information (NCEI). https://www.ncdc.noaa.gov/teleconnections/enso/.
49. Curtis, S., Adler, R., Curtis, S. & Adler, R. ENSO Indices Based on Patterns of Satellite-Derived

Precipitation. *http://dx.doi.org/10.1175/1520-0442(2000)013<2786:EIBOPO>2.0.CO;2* (2000) doi:10.1175/1520-0442(2000)013<2786:EIBOPO>2.0.CO;2.

50. Christensen, J. H. *et al.* Climate phenomena and their relevance for future regional climate change. *Clim. Chang. 2013 Phys. Sci. Basis Work. Gr. I Contrib. to Fifth Assess. Rep. Intergov. Panel Clim. Chang.* **9781107057**, 1217–1308 (2013).
51. Gutiérrez, O. *et al.* Climate teleconnections and indicators of coastal systems response. *Ocean Coast. Manag.* **122**, 64–76 (2016).
52. Enfield, D. B., Mestas-Nuñez, A. M. & Trimble, P. J. The Atlantic Multidecadal Oscillation and its relation to rainfall and river flows in the continental U.S. *Geophys. Res. Lett.* **28**, 2077–2080 (2001).
53. JISAO. Arctic Oscillation (AO). http://research.jisao.washington.edu/data/aots/.
54. NOAA. Climate Prediction Center - Arctic Oscillation. https://www.cpc.ncep.noaa.gov/products/precip/CWlink/daily_ao_index/ao.shtml.
55. NOAA. North Atlantic Oscillation (NAO). 1–2 (2015).
56. NOAA. Climate Prediction Center - Northern Hemisphere Teleconnection Patterns. https://www.cpc.ncep.noaa.gov/data/teledoc/telecontents.shtml.
57. NOAA. Climate Prediction Center - Monitoring & Data: Current Monthly Atmospheric and Sea Surface Temperatures Index Values. https://www.cpc.ncep.noaa.gov/data/indices/.
58. Trenberth, K. E. & Hurrell, J. W. Decadal atmosphere-ocean variations in the Pacific. *Clim. Dyn.* **9**, 303–319 (1994).
59. JISAO. Pacific Decadal Oscillation (PDO). in doi:10.4135/9781446247501.n2786.
60. Mantua, N. J. *et al.* A Pacific Interdecadal Climate Oscillation with Impacts on Salmon Production**. *https://doi.org/10.1175/1520-0477(1997)078<1069:APICOW>2.0.CO;2* (1997) doi:10.1175/1520-0477(1997)078<1069:APICOW>2.0.CO;2.
61. Zhang, Y. *et al.* ENSO-like Interdecadal Variability: 1900–93. *http://dx.doi.org/10.1175/1520-0442(1997)010<1004:ELIV>2.0.CO;2* (1997) doi:10.1175/1520-0442(1997)010<1004:ELIV>2.0.CO;2.
62. Revelle, W. *Package ' psych '*. https://personality-project.org/r/psych (2019).
63. MM, M. Statistics Corner: A guide to appropriate use of Correlation coefficient in medical research. *Malawi Med. J.* **24**, 69–71 (2012).
64. Asuero, A. G., Sayago, A. & González, A. G. The correlation coefficient: An overview. *Crit. Rev. Anal. Chem.* **36**, 41–59 (2006).
65. Taylor, R. Interpretation of the Correlation Coefficient: A Basic Review. *J. Diagnostic Med. Sonogr.* **6**, 35–39 (1990).
66. Dolan, R., Fenster, M. S. & Holme, S. J. Temporal Analysis of Shoreline Recession and Accretion. *Source J. Coast. Res.* **721528**, 723–744 (1991).
67. Corbella, S. & Stretch, D. D. D. Decadal trends in beach morphology on the east coast of South Africa and likely causative factors. *Nat. Hazards Earth Syst. Sci.* **12**, 2515–2527 (2012).
68. Socioeconomic Data and Applications Center (SEDAC)CIESIN, Earth Institute at Columbia University Palisades, N. Y. ciesin. columbia. eduNationa. A. and S. A. Low-Elevation Coastal Zone (LECZ). 2016 (2016).
69. Burke, L. & Sugg, Z. Hydrologic Modeling of Watersheds Discharging Adjacent to the Mesoamerican Reef. *World Resour. Inst.* 35 (2006).
70. Berger, W. H., Lange, C. B. & Wefer, G. Upwelling history of the Benguela-Namibia system: A synthesis of Leg 175 results. *Proc. Ocean Drill. Progr. Sci. Results* **175**, 1–53 (2002).
71. Andel, V. & G, T. S. Marine Geology of the Gulf of California. *Limnol. Oceanogr.* **10**, 303–304 (1965).
72. Glenn, E. P., Flessa, K. W. & Pitt, J. Restoration potential of the aquatic ecosystems of the Colorado River Delta, Mexico: Introduction to special issue on 'Wetlands of the Colorado River Delta'. *Ecol. Eng.* **59**, 1–6 (2013).
73. Pitt, J. Shaping the 2014 Colorado River Delta pulse flow: Rapid environmental flow design for

ecological outcomes and scientific learning. *Ecol. Eng.* **106**, 704–714 (2017).
74. Stănică, A., Panin, N., Staˇnicaˇ, A. & Panin, N. Present evolution and future predictions for the deltaic coastal zone between the Sulina and Sf. Gheorghe Danube river mouths (Romania). *Geomorphology* **107**, 41–46 (2009).
75. Claudino-Sales, V. Danube Delta, Romania. in *Coastal Research Library* vol. 28 93–97 (2019).
76. Ionescu, I. & Noaje, I. Natural environment change detection in Danube Delta, based on HRV - SPOT images. *Int. J.* (1993).
77. Dan, S. *Coastal Dynamics of the Danube Delta*. (2013). doi:10.4233/uuid:9c19651e-e744-43c3-aa85-7ea7abd14a2.
78. Kunz, H. Groynes on the East Frisian Islands: History and Experiences. in *Coastal Engineering 1996* 2128–2141 (American Society of Civil Engineers, 1997). doi:10.1061/9780784402429.165.
79. Winter, C. Macro scale morphodynamics of the German North Sea coast. *J. Coast. Res.* **n SPEC. IS**, 706–710 (2011).
80. Trilateral Working Group on Coastal Protection and Sea Level Rise. *CPSL Third Report*. *Wadden Sea Ecosystem* vol. 28 (2010).
81. Trilateral Working Group on Coastal Protection and Sea Level Rise. *Coastal Protection and Sea Level Rise: solutions for sustainable coastal protection in the Wadden Sea Region*. *Zhurnal Eksperimental'noi i Teoreticheskoi Fiziki* http://scholar.google.com/scholar?hl=en&btnG=Search&q=intitle:No+Title#0 (2005).
82. Moser, M. & Brown, A. Trilateral Wadden Sea Cooperation External Evaluation Report. (2007).
83. Mulder, J. P. M., Hommes, S. & Horstman, E. M. Implementation of coastal erosion management in the Netherlands. *Ocean Coast. Manag.* **54**, 888–897 (2011).
84. Elias, E. P. L. & Van Der Spek, A. J. F. Dynamic preservation of Texel Inlet, the Netherlands: Understanding the interaction of an ebb-tidal delta with its adjacent coast. *Geol. en Mijnbouw/Netherlands J. Geosci.* **96**, 293–317 (2017).
85. Mehvar, S., Filatova, T., Dastgheib, A., de Ruyter van Steveninck, E. & Ranasinghe, R. Quantifying Economic Value of Coastal Ecosystem Services: A Review. *J. Mar. Sci. Eng.* **6**, 5 (2018).
86. Reguero, B. G., Beck, M. W., Agostini, V. N., Kramer, P. & Hancock, B. Coral reefs for coastal protection: A new methodological approach and engineering case study in Grenada. *J. Environ. Manage.* **210**, 146–161 (2018).
87. Harris, D. L. *et al.* Coral reef structural complexity provides important coastal protection from waves under rising sea levels. *Sci. Adv.* **4**, 1–8 (2018).
88. Heron, S. F. *et al.* Impacts of Climate Change on World Heritage Coral Reefs: A First Global Scientific Assessment. *Paris, UNESCO World Herit. Centre.* 1–14 (2017).
89. Hoegh-Guldberg, O. *et al. Impacts of 1.5°C of Global Warming on Natural and Human Systems*. https://www.ipcc.ch/site/assets/uploads/sites/2/2019/02/SR15_Chapter3_Low_Res.pdf (2018).
90. Hoegh-guldberg, O., Kennedy, E. V, Beyer, H. L., Mcclennen, C. & Possingham, H. P. Securing a Long-term Future for Coral Reefs. *Trends Ecol. Evol.* **33**, 936–944 (2018).
91. Zaneveld, J. R. *et al.* Overfishing and nutrient pollution interact with temperature to disrupt coral reefs down to microbial scales. *Nat. Commun.* **7**, 1–12 (2016).
92. Richards, J. A. & Richards, J. A. Error Correction and Registration of Image Data. *Remote Sens. Digit. Image Anal.* 39–74 (1993) doi:10.1007/978-3-642-88087-2_2.
93. Zheng, X., Huang, Q., Wang, J., Wang, T. & Zhang, G. Geometric accuracy evaluation of high-resolution satellite images based on Xianning test field. *Sensors (Switzerland)* **18**, 1–11 (2018).
94. Cazenave, A. & Cozannet, G. Le. Sea level rise and its coastal impacts. *Earth's Futur.* **2**, 15–34 (2013).
95. Pickering, M. D. *et al.* The impact of future sea-level rise on the global tides. *Cont. Shelf Res.* **142**, 50–68 (2017).

96. Leatherman, S. P., Zhang, K. & Douglas, B. C. Sea level rise shown to drive coastal erosion. *Eos (Washington. DC).* **81**, 55–57 (2000).

97. De Jong, F. *et al.* Wadden Sea Quality Status Report - Geomorphology. *Wadden Sea Ecosyst.* **9**, (1999).

98. Nicholls, R. J. Assessing erosion of sandy beaches due to sea-level rise. *Geol. Soc. Eng. Geol. Spec. Publ.* **15**, 71–76 (1998).

99. Le Cozannet, G., Garcin, M., Yates, M., Idier, D. & Meyssignac, B. Approaches to evaluate the recent impacts of sea-level rise on shoreline changes. *Earth-Science Rev.* **138**, 47–60 (2014).

100. Reise, K. Coast of change: Habitat loss and transformations in the Wadden Sea. *Helgol. Mar. Res.* **59**, 9–21 (2005).

101. Benninghoff, M. & Winter, C. Recent morphologic evolution of the German Wadden Sea. *Sci. Rep.* **9**, 1–9 (2019).

102. Lotze, H. K. *et al.* Human transformations of the Wadden Sea ecosystem through time: A synthesis. *Helgol. Mar. Res.* **59**, 84–95 (2005).

103. Becherer, J. *et al.* The Wadden Sea in transition - consequences of sea level rise. *Ocean Dyn.* **68**, 131–151 (2018).

104. Perry, J. Climate change adaptation in natural world heritage sites: A triage approach. *Climate* **7**, (2019).

105. Bottrill, M. C. *et al.* Is conservation triage just smart decision making? *Trends Ecol. Evol.* **23**, 649–654 (2008).

106. Salm, R. V. & Clark, J. R. *Marine and Coastal Protected Areas: A guide for Planners and Managers*. (2010).